DOI: 10.1002/chem.200600302

# Noncovalent Functionalization and Solubilization of Carbon Nanotubes by Using a Conjugated Zn–Porphyrin Polymer

**Fuyong Cheng and Alex Adronov*[a]**

**Abstract:** A highly soluble, conjugated Zn–porphyrin polymer was synthesized and found to strongly interact with the surface of single-walled carbon nanotubes, producing a soluble polymer–nanotube complex. Successful complexation required the addition of trifluoroacetic acid to the solvent (THF). It was found that the complex remained soluble after excess free polymer was removed from solution, and could be centrifuged at high speed with no observable sedimentation. Furthermore, the polymer–nanotube assembly resulted in enhanced planarization and conjugation within the porphyrin polymer, which was manifested in a 127 nm bathochromic shift of the Q-band absorption. Control experiments with the Zn–porphyrin monomer indicated that homogeneous solutions could be prepared by means of sonication, but the monomer–nanotube interactions were significantly weaker, leading to nanotube precipitation within minutes. Atomic force microscopy (AFM) studies indicated that the polymer enables exfoliation of nanotube bundles and is able to "stitch" multiple nanotubes together into a series of long, interconnected strands.

**Keywords:** absorption spectroscopy · atomic force microscopy · nanotubes · noncovalent interactions · polymers

## Introduction

The functionalization and subsequent dissolution of single-walled carbon nanotubes (SWNTs) has received significant attention over the past several years and has resulted in the development of a number of functionalization methods. These methods can be divided into two broad categories, namely, covalent and noncovalent (supramolecular) approaches.[1–5] Covalent functionalization has been widely investigated, and has produced an array of modified nanotube structures bearing both small molecules and polymers.[6–10] However, this strategy significantly perturbs the conjugated π system of a carbon nanotube and can result in dramatic changes in its electronic and structural properties.[11,12] Therefore, covalently modified SWNTs may not be suitable in applications that rely on the high conductivity or mechanical strength of SWNTs. Conversely, the supramolecular method involves physical adsorption of molecules capable of π-stacking or van der Waals interactions with the conjugated aromatic nanotube sidewall. This strategy preserves the electronic and structural integrity of SWNTs, permitting the use of both their conductivity and strength properties in eventual applications. For this reason, noncovalent attachment of numerous aromatic species to the nanotube surface has been investigated.[13–28] Most notably, conjugated polymers such as poly(phenylenevinylene)[17–19] and poly(aryleneethynylene),[21] as well as small aromatic molecules such as pyrene,[13–16,20] anthracene,[22] and phthalocyanine[23] derivatives that bind to SWNTs through π-stacking interactions have been used to decorate the nanotube surface and modify solubility and electronic properties. More recently, supramolecular functionalization of nanotubes with porphyrins has been increasingly investigated[24–29] because these flat, planar aromatic structures are ideal for π-stacking interactions with the aromatic sidewalls of SWNTs and they exhibit unique photophysical and electrochemical properties.[30] Nakashima and co-workers were first to show that Zn–protoporphyrins (ZnPP) can bind to the SWNT surface, resulting in stable nanotube–ZnPP solutions in DMF as long as excess porphyrin is present in solution.[24] However, upon removal of excess ZnPP, it was found that the nanotube–ZnPP complex precipitates within a few days. Sun and co-

[a] Dr. F. Cheng, Prof. Dr. A. Adronov
Department of Chemistry
McMaster University
Hamilton, Ontario L8S 4M1 (Canada)
Fax: (+1) 905-521-2773
E-mail: adronov@mcmaster.ca

Supporting information for this article is available on the WWW under http://www.chemeurj.org/ or from the author.

  

workers have reported selective interactions of porphyrins with SWNTs, allowing the separation of semiconducting nanotubes from metallic nanotubes.[25] Again, removal of excess porphyrin from solution resulted in the recovery of insoluble SWNTs, indicating that the SWNT–porphyrin complex could easily be dissociated. Also in their work, it was found that free-base porphyrins interacted with SWNTs in THF, but Zn–porphyrins exhibited no solubilizing interactions (a result somewhat contradictory to that of Nakashima). Additionally, Kamat and co-workers reported the use of protonated porphyrins to assemble SWNTs into supramolecular porphyrin–nanotube aggregates.[27] These macroscopic nanotube bundles could be suspended in THF by means of sonication, but were easily sedimented by centrifugation, indicating a lack of molecular-level solubility.

Building on these results, we were interested in examining macromolecular structures bearing multiple porphyrin units in an attempt to increase the interaction strength through multivalent binding. Conjugated porphyrin polymers containing butadiyne bridges linked directly to the porphyrin *meso*-carbon atoms, first reported by Anderson et al.,[31] exhibit unique spectroscopic and redox properties that make them promising candidates for applications in nonlinear optics and molecular electronics.[32,33] The fully conjugated, rigid structure of these polymers, coupled with their strong electron-donating properties, make them highly complementary to the conjugated, rigid, but electron-accepting SWNTs.[34] It was therefore reasonable to expect that the interaction between SWNTs and conjugated porphyrin polymers would be much stronger than the analogous interaction with monomeric porphyrins. To date, only three examples of soluble, conjugated porphyrin-containing polymers have been reported, each of which was rendered soluble by aliphatic side chains linked via ester[31] or amide[32] bonds. Here we report the synthesis of a highly stable and soluble Zn–porphyrin polymer that has three hexadecyl branches linked via robust ether bonds to the aryl substituents on both of the porphyrin *meso* positions. It was found that, although this target polymer was composed of Zn–porphyrins rather than free-base porphyrins, it nevertheless exhibited strong interactions with the nanotube surface in THF upon addition of small quantities of trifluoracetic acid (TFA). This interaction resulted in porphyrin coplanarization and a consequent increase in the effective conjugation within the polymer (Figure 1). The increased conjugation leads to a greater degree of electron delocalization and a smaller HOMO–LUMO gap, which results in a large bathochromic shift of the Q band in the polymer absorption spectrum.

## Results and Discussion

**Synthesis and characterization**: Synthesis of the target porphyrin polymer **2** was accomplished through minor modification of previously published procedures (Scheme 1).[33] Briefly, treatment of commercially available methyl 3,4,5-trihydroxybenzoate with three equivalents of 1-bromohexadecane resulted in methyl 3,4,5-tris(hexadecyloxy)benzoate (**3**), which was reduced with $LiAlH_4$ and subsequently oxidized with $MnO_2$ to give aldehyde **5** in a 74% yield (over three steps). Subsequent treatment of **5** with pyrrole, followed by condensation with trimethylsilylpropynal and metalation with $Zn^{II}$ acetate afforded the trimethylsilyl (TMS)-protected monomer, which was deprotected with tetrabutylammonium fluoride (TBAF) to produce the target monomer **1** (24% yield over four steps). Metalation of the monomer with Zn is important as it improves the stability of the porphyrin, allows polymerization to occur cleanly without catalyst coordination/deactivation (known to occur with free-base porphyrins), and improves the solubility of the product in coordinating solvents such as THF. The Glaser–Hay coupling of monomer **1** using CuCl and *N*,*N*,*N*′,*N*′-tetramethylethylenediamine (TMEDA) in $CH_2Cl_2$/1% pyridine resulted in rapid polymerization at room temperature, allowing the isolation of polymer **2** in a 90% yield.

The $^1H$ NMR spectrum of polymer **2** in $CDCl_3$ exhibited all the expected signals for the polymer repeat units and confirmed the disappearance of terminal alkyne protons at

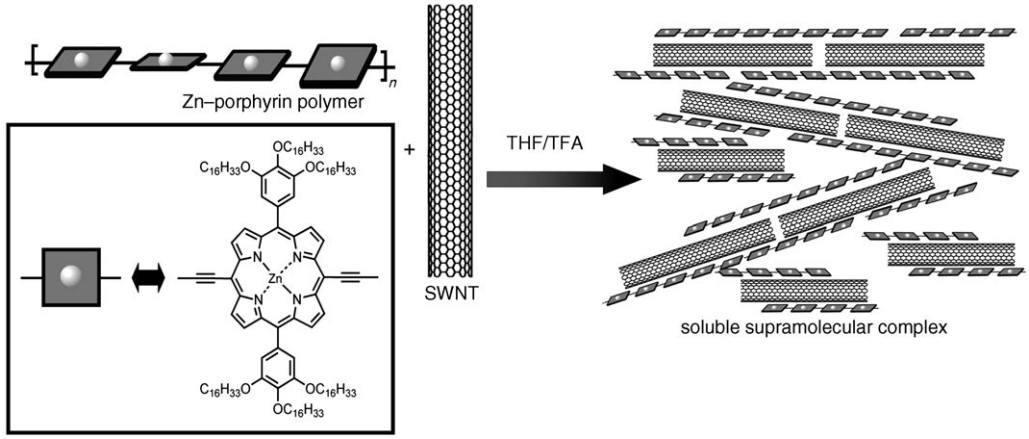


Figure 1. Supramolecular assembly of the conjugated Zn–porphyrin polymer with SWNTs, forming a soluble polymer–nanotube complex.

  

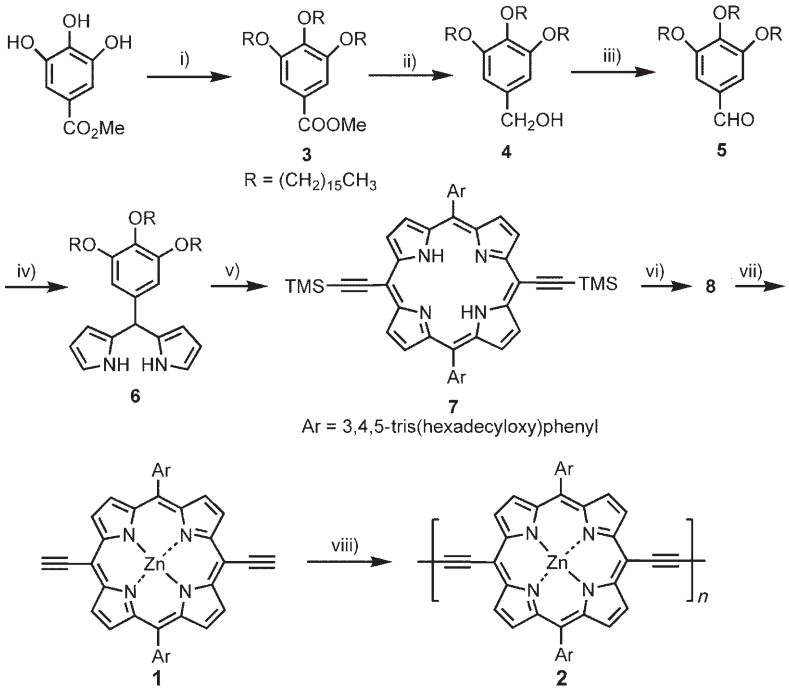


Scheme 1. Synthesis of **2**. Conditions: i) RBr, $K_2CO_3$, KI, DMF, 85%; ii) $LiAlH_4$, THF, 88%; iii) $MnO_2$, $CH_2Cl_2$, 99%; iv) pyrrole, $CH_2Cl_2$, 95%; v) 3-trimethylsilylpropynal, $BF_3{\cdot}OEt_2$, DDQ, $CH_2Cl_2$, 28%; vi) $Zn(OAc)_2$, $CHCl_3$/MeOH, 95%; vii) TBAF, $CH_2Cl_2$, 96%; viii) CuCl, TMEDA, $CH_2Cl_2$/pyridine, 90%.

$\delta = 4.16$ ppm (see the Supporting Information). Gel permeation chromatography (GPC), relative to polystyrene standards, resulted in a polymer number-average molecular weight ($M_n$) of 45700 g mol$^{-1}$, with a polydispersity of 1.93, in accordance with previous examples of similar polymerization reactions.[32,33] Because it is well known that GPC analysis of rigid-rod polymers using polystyrene standards can overestimate the molecular weight,[35] we compared our results with those obtained from GPC analyses of monomer **1**. The monomer gave an $M_n$ value of 3250 g mol$^{-1}$, which is higher than the theoretical molar mass of 2016.51 g mol$^{-1}$ for this compound. We therefore estimate that the degree of polymerization for **2** was approximately 14 repeat porphyrin units. Unfortunately, all our attempts to perform matrix-assisted laser desorption/ionization time-of-flight (MALDI-TOF) mass spectrometry (MS) on polymer **2** resulted in no observable signal, presumably due to the difficulty of transferring the polymer structures into the gas phase. Based on the GPC data and previous molecular modeling and crystallography studies,[36] the average length of the polymer was estimated to be approximately 18 nm. Polymer **2** was found to be highly soluble in $CH_2Cl_2$ and $CHCl_3$ in the presence of small quantities of pyridine (1% v/v). However, this polymer was most soluble in THF, in which coordination of the furan oxygen to the polymer Zn atoms greatly diminishes polymer aggregation and facilitates dissolution.[33]

The UV spectrum of polymer **2** closely resembles that of previously reported polymers of this type (see Figure S3 in the Supporting Information).[32,33] It reveals a broadened Soret band at 468 nm and a long-wavelength Q band, which shifts from 625 nm in monomer **1** to 793 nm in polymer **2**, caused by the extended conjugation and significant electronic communication between the porphyrin repeat units. Additionally, the polymer exhibits a broad fluorescence emission band at 816 nm, whereas the monomer emits at 638 and 691 nm. This further confirms that the polymer has a much smaller HOMO–LUMO gap than that of the monomer.

**Supramolecular interactions with SWNTs**: The observed electronic and structural properties of the polymer encouraged us to study its supramolecular interactions with SWNTs. In all of the studies, the SWNTs, prepared by the high-pressure carbon monoxide (HiPco) disproportionation process, were used as purchased without further treatment. As polymer **2** was found to be most soluble in THF, this was chosen as the optimal solvent for investigating the supramolecular interactions with the SWNTs. Unfortunately, mixing and sonication of **2** and the SWNTs in THF resulted in no observable nanotube solubility, consistent with previous observations of Sun and co-workers.[25] It was postulated that coordination of THF to the Zn–porphyrin repeat units prohibits the polymer from closely interacting with the carbon-nanotube surface. However, when the same experiment was conducted in acidified THF, containing 5% trifluoroacetic acid (TFA) (v/v), we were surprised to observe a high degree of nanotube solubility, reaching close to 1 mg mL$^{-1}$. In a typical experiment, a sample of SWNTs (10 mg) was added to a solution of **1** or **2** (30 mg) in acidified THF (10 mL). The resulting suspension was sonicated for one hour at room temperature and then diluted with a further 50 mL of the acidified THF. This produced a homogeneous solution that was then filtered through a 450 nm-pore Teflon membrane and was repeatedly washed with acidified THF until the filtrate was colorless; this indicated the removal of all excess porphyrin monomer **1** or polymer **2**. The residue was then collected and the solid was resuspended in acidified THF (10 mL) with sonication for five minutes. When this procedure was carried out with monomer **1**, a homogeneous solution initially formed, but this solution was not stable and the SWNTs precipitated after standing for a few minutes (Figure 2B). In contrast, when polymer **2** was used, a very dark and stable solution was obtained after sonication for 5 min (Figure 2D), leaving practically no observable insoluble nanotube residue. This solution remained stable

  

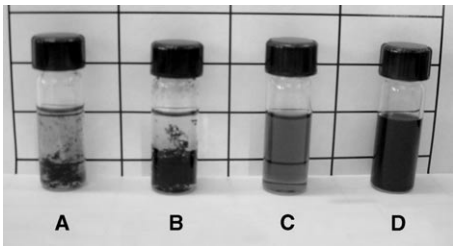


Figure 2. Photograph of four samples in acidified THF (containing 5% TFA): A) pristine full-length SWNTs; B) monomer **1**/SWNT mixture; C) polymer **2**; D) polymer **2**/SWNT mixture, which forms a dark, homogeneous solution.

upon standing for several weeks, with no sedimentation even after centrifugation for 20 min at 5000 rpm. This result indicates that the multivalent polymer–nanotube interaction is very strong, and allows the retention of significant amounts of polymer bound to the nanotube surface even after excess unbound polymer has been removed.[37] Clearly, the flat, planar aromatic porphyrins are responsible for the binding strength, while the six long aliphatic chains appended to each porphyrin repeat unit impart a high degree of solubility. The fact that porphyrin polymer **2** can be used to form a very stable and highly soluble polymer–SWNT composite, whereas the monomeric porphyrin results in an unstable suspension, implies that multivalent binding and the enhanced π conjugation of polymer **2** are responsible for strengthening the supramolecular nanotube interactions. As an additional control experiment, when only the SWNTs were suspended in acidified THF under the conditions outlined above, nanotube solubility was not observed to any extent.

Formation of the polymer–SWNT complex is also evident from changes in the UV-visible spectrum of the polymer. Figure 3 shows the absorption spectra of polymer **2** in THF, polymer **2** in acidified THF, unfunctionalized SWNTs in DMF, and the polymer **2**–SWNT complex in acidified THF.

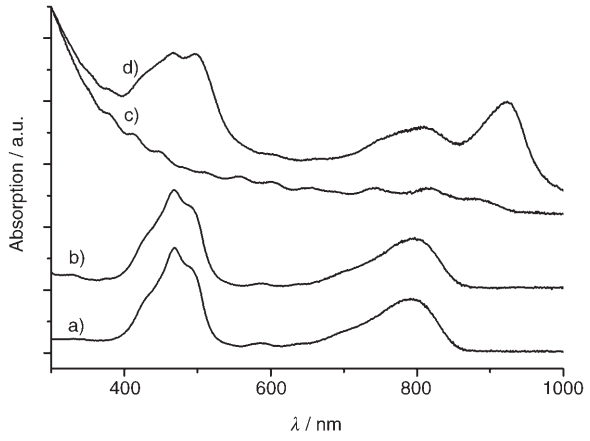


Figure 3. UV/Vis absorption spectra of a) **2** in THF, b) **2** in acidified THF, c) SWNTs in DMF, and d) the mixture of polymer **2** and SWNTs in acidified THF. a.u. = arbitrary units.

Notably, the absorption of **2** in acidified THF was almost identical to that in neat THF, which suggests that TFA neither changes the electronic structure of the polymer, nor affects the Zn ions coordinated to the porphyrin repeat units.[38] The exact role of TFA in promoting supramolecular interactions between SWNTs and the zinc–porphyrin polymer is not fully understood and is currently under investigation. Nevertheless, the interaction between polymer **2** and the SWNTs is evident from changes in the Soret and Q bands of the polymer in the polymer–SWNT complex. Figure 3d displays an increase in the intensity of the longer wavelength shoulder of the Soret band, shifting the $\lambda_{max}$ from 467 to 498 nm. Additionally, the Q band shifted from 796 to 923 nm in the complex. However, the absorption spectrum of the polymer–nanotube complex also exhibits absorption bands at 467 and 796 nm, corresponding to free polymer in solution. Clearly, the inherent solubility of the polymer results in some polymer chains desorbing from the nanotube surface, thus creating an equilibrium between free and bound polymer in solution.

The origin of the absorption red-shifts in the UV-visible spectrum of the polymer–SWNT complex is likely a coplanarization of the porphyrins in the polymer. It is known that there is no steric barrier to rotation about the butadiyne links in the porphyrin polymer structure, which allows the free polymer to adopt conformations that are not entirely coplanar.[32,33] Anderson and co-workers applied bidentate ligands, such as 4,4′-bipyridine or 1,4-diazabicyclo-[2.2.2]octane (DABCO), to form a double-stranded ladder complex with porphyrin polymers.[33] It was found that this self-assembly process restricts the porphyrin rotation about the butadiyne links, which increases the coplanarity between neighboring porphyrins along the polymer chain. This increased coplanarity extends the π-conjugation length, resulting in a redshift of the electronic absorption spectrum by 75 nm. In our supramolecular nanotube assembly, a similar coplanarity induction is likely achieved due to the rigid nanotube sidewall structure. Here, the nanotube acts as a template that restricts torsional disorder within the polymer backbone and induces a coplanar arrangement of porphyrin repeat units (for a schematic illustration, see Figure 1). The consequent extension of π conjugation is manifested in the observed large absorption redshift of 127 nm.

The soluble polymer–SWNT complex was also investigated by using atomic force microscopy (AFM). Several drops of the polymer–nanotube solution in acidified THF were spin coated onto freshly cleaved mica. Figure 4A depicts an amplitude image of this sample obtained by tapping mode AFM. It is clear that numerous features resembling nanotube-containing structures are observable on the substrate. Based on height profile analysis, it seems that these structures are mostly individual nanotubes coated with the porphyrin polymer. This can be more clearly seen in the higher-magnification height image (Figure 4B), in which a range of heights was observed for different strands corresponding to a progression from a few single, uncoated SWNT segments (i) exhibiting heights of approximately 1 nm, to polymer-

  

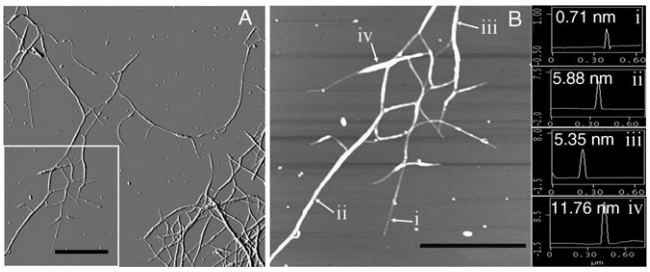


Figure 4. AFM images (scale bars≅1 μm) of polymer–SWNT complexes spin cast from acidified THF. A) AFM amplitude image of the SWNT–polymer complex on freshly cleaved mica (white box indicates region magnified in B). B) Higher magnification AFM height image showing the polymer coating on nanotube strands (white); arrows indicate locations where cross-sectional analysis was performed to determine feature heights, shown at right.

coated SWNTs (ii, iii) that make up the majority of the observed features with heights of approximately 5 to 6 nm. These values are consistent with estimated dimensions of a single SWNT coated with polymer **2** (see Figure S5 in the Supporting Information). Interestingly, the height analysis of some thicker regions (such as iv) indicates heights in the range of 10 to 12 nm, which match well with the expected height of two overlapping polymer-coated nanotubes. In some regions, heights corresponding to three or more overlapping nanotubes were also found. These observations indicate that sonication in the presence of polymer **2** allows debundling of SWNTs to some extent, and the stabilization of individual nanotubes in solution. In addition, the AFM image indicates that polymer-coated nanotubes form long, interconnected strands. Considering that the nanotubes, on average, range in length from 0.5 to 3 μm, it seems that the porphyrin polymers are capable of "stitching" individual nanotubes together into a series of long, interconnected nanofibers that span distances of more than 5 μm (Figure 4A).

## Conclusion

Highly soluble, conjugated porphyrin polymers are capable of strong supramolecular interactions with SWNTs and result in the formation of very stable and highly soluble polymer–SWNT nanocomposites. It was found that addition of TFA to the polymer–nanotube solution greatly enhanced the supramolecular interaction. The polymer–nanotube assembly process induces a coplanarization in the polymer repeat units, causing enhanced conjugation and a 127 nm bathochromic shift of the Q-band absorption. In addition, AFM studies indicate that the polymer can exfoliate nanotube bundles and "stitch" multiple nanotubes together into long strands. The broad absorption spectrum of the polymer–nanotube complex, ranging from the UV to the near-IR, coupled with the high nanotube solubility, opens this novel supramolecular system to potential applications in the development of light-harvesting photovoltaic systems and other optoelectronic devices.

## Experimental Section

**General**: Single-walled carbon nanotubes (SWNTs) were purchased from Carbon Nanotechnologies, Inc. (Houston, TX). All reagents and solvents were purchased from commercial suppliers and used as received. Atomic force microscopy was carried out by using a Digital Instruments NanoScope IIIa Multimode AFM, with samples prepared by spin coating (2500 rpm) onto freshly cleaved mica substrates. The images were recorded with standard tips in the tapping mode at a scan rate of 1.0 Hz. FTIR analyses were performed on a BIO-RAD FTS-40 instrument. NMR spectroscopy was performed on a Bruker 200, 500, or 600 MHz instrument. UV-visible spectra were measured by using a Cary 50 UV-visible spectrophotometer. Ultrasonication was carried out in a Banson Ultrasonics B1510 bath sonicator. High-resolution (HR) electrospray ionization (ESI) MS measurements were carried out on the Micromass Ultima Global instrument (quadrupole time-of-flight) and high-resolution MALDI-MS analyses were performed on the Waters/Micromass MALDI Micro instrument (α-cyano-4-hydroxycinnamic acid as the matrix). Filtration was performed through a 450 nm-pore Teflon membrane (Millipore). Polymer molecular weight and polydispersity index (PDI) were estimated from gel permeation chromatography (GPC) analyses by using a Waters 2695 Separations Module equipped with a Waters 2996 photodiode array detector, a Waters 2414 refractive-index detector, a Waters 2475 Multi-λfluorescence detector, and four Polymer Labs PLgel individual pore-size columns. Polystyrene standards were used for calibration, and THF was used as the eluent at a flow rate of 1.0 mL min$^{-1}$.

**Synthesis**

**Methyl 3,4,5-tris(hexadecyloxy)benzoate (3)**: A mixture of trihydroxylbenzoate methylester (10.0 g, 54 mmol), 1-bromohexadecane (100.0 g, 328 mmol, 6 equiv), $K_2CO_3$ (89.0 g, 648 mmol, 12 equiv), and KI (27.0 g, 162 mmol, 3 equiv) in DMF (1 L) was heated at reflux for 24 h under an argon atmosphere. The DMF was evaporated under vacuum and the crude product was dissolved in $CH_2Cl_2$ (1 L), and washed with water. The solvent was evaporated under vacuum and the residue was dissolved in a minimum of $CH_2Cl_2$ and precipitated into MeOH. Upon filtration, washing with MeOH, and drying, a white powder was obtained (40.0 g, 85%). $^1$H NMR ($CDCl_3$, 200 MHz): $\delta = 0.87$ (t, $J = 6.71$ Hz, 9H), 1.25–1.30 (m, 39H), 1.40–1.55 (m, 6H), 1.65–1.85 (m, 6H), 3.88 (s, 3H), 4.00 (t, $J = 6.36$ Hz, 6H), 7.24 ppm (s, 2H); $^{13}$C NMR ($CDCl_3$, 50 MHz): $\delta = 14.1$, 22.7, 26.1, 29.3, 29.7, 30.3, 31.9, 52.1, 69.1, 73.5, 107.9, 124.6, 142.3, 152.8, 166.4 ppm; IR (KBr): $\tilde{\nu} = 2920$, 2853 ($CH_2$), 1719 (C=O), 1220, 1118 cm$^{-1}$ (C–O); HRMS (ESI): $m/z$ calcd for $C_{56}H_{104}O_5$ $[M]^+$: 856.7884; found: 856.7865.

**3,4,5-Tris(hexadecyloxy)benzyl alcohol (4)**: Compound **3** (33.0 g, 38.5 mmol) in anhydrous THF (200 mL) was added dropwise to a suspension of $LiALH_4$ (3.66 g, 96.2 mmol) in anhydrous THF (100 mL) at 0°C. Then the resulting mixture was warmed to room temperature, stirred for 2 h, and re-cooled to 0°C before water was added to quench the excess of $LiALH_4$. The mixture was extracted with $CH_2Cl_2$ (100 mL) followed by additional $CH_2Cl_2$ (2×50 mL). The combined extracts were washed with $H_2O$ (3×100 mL) dried over $Na_2SO_4$, and filtered. The filtrate was evaporated to dryness and **4** was obtained as a white solid (28.0 g, 88%). $^1$H NMR ($CDCl_3$, 200 MHz): $\delta = 0.87$ (t, $J = 6.71$ Hz, 9H), 1.25–1.30 (m, 39H), 1.46–1.50 (m, 6H), 1.67–1.82 (m, 6H), 3.89–3.99 (m, 6H), 4.58 (d, $J = 5.51$ Hz, 2H), 6.55 ppm (s, 2H); $^{13}$C NMR ($CDCl_3$, 50 MHz): $\delta = 14.1$, 22.7, 26.1, 29.4, 29.7, 30.3, 31.9, 65.7, 69.1, 73.4, 105.3, 136.0, 138.1, 153.3 ppm; IR (KBr): $\tilde{\nu} = 3416$ (O–H), 2920, 2852 cm$^{-1}$ ($CH_2$); HRMS (ESI): $m/z$ calcd for $C_{55}H_{105}O_4$ $[M+1]^+$: 829.8013; found: 829.8050.

**3,4,5-Tris(hexadecyloxy)benzaldehyde (5)**: Activated $MnO_2$ (40 g, 0.46 mol) was added to a solution of **4** (20.0 g, 24.1 mmol) in anhydrous $CH_2Cl_2$ (300 mL) at room temperature, and the resulting suspension was stirred for 6 h. The reaction mixture was filtered through Celite with $CH_2Cl_2$ (5×50 mL) as the eluent. The solvent was removed under

  

vacuum to give compound **5** as a white powder (20.0 g, 99%). $^1$H NMR ($CDCl_3$, 200 MHz): $\delta = 0.87$ (t, $J = 6.71$ Hz, 9H), 1.25–1.30 (m, 39H), 1.46–1.50 (m, 6H), 1.62–1.86 (m, 6H), 4.08–3.99 (m, 6H), 7.08 (s, 2H), 9.83 ppm (s, 1H); $^{13}$C NMR ($CDCl_3$, 50 MHz): $\delta = 14.1$, 22.7, 26.1, 29.4, 29.7, 30.4, 31.9, 69.2, 73.6, 107.8, 131.4, 143.8, 153.5, 191.3 ppm; IR (KBr): $\tilde{\nu} = 2917$, 2849 ($CH_2$), 1693 cm$^{-1}$ (C=O); HRMS (ESI): *m*/*z* calcd for $C_{55}H_{102}O_4$ $[M]^+$: 826.7778; found: 826.7795.

**2,2′-{[3,4,5-Tris(hexadecyloxy)phenyl]methylene}bis(1*H*-pyrrole) (6)**: A solution of **5** (20.0 g, 8.62 mmol) in pyrrole (200 mL) was degassed by bubbling with Ar for 30 min, and then TFA (0.6 mL) was added. The solution was stirred for 15 min at room temperature, then was diluted with $CH_2Cl_2$ (300 mL), washed with 0.1 M NaOH (100 mL), water (3× 100 mL), dried over $Na_2SO_4$, and filtered. After removal of the low-boiling solvent, the excess pyrrole was recovered by distillation under vacuum, and the residue was dissolved in $CH_2Cl_2$ (100 mL) and precipitated by addition of MeOH. The resulting suspension was filtered and dried under vacuum, resulting in a white powder (21.5 g, 95%). $^1$H NMR ($CDCl_3$, 200 MHz): $\delta = 0.86$ (t, $J = 6.71$ Hz, 9H), 1.24–1.32 (m, 39H), 1.46–1.50 (m, 6H), 1.68–1.86 (m, 6H), 3.81–3.90 (m, 6H), 5.41 (s, 1H), 5.90 (m, 2H), 6.16 (m, 2H), 6.71 (m, 2H), 6.80 (s, 2H), 8.15 ppm (brs, 2H); $^{13}$C NMR spectra of **6** could not be adequately measured because **6** was found to be unstable in solution over the duration of the measurement; IR (KBr): $\tilde{\nu} = 2919$, 2851 ($CH_2$), 1116 cm$^{-1}$ (C–O); HRMS (ESI): *m*/*z* calcd for $C_{63}H_{111}N_2O_3$ $[M+1]^+$: 943.8595; found: 943.8608.

**5,15-Bis[3,4,5-tris(hexadecyloxy)phenyl]-10,20-bis[2-(trimethylsilyl)ethynyl]porphyrin-*N*$^{21}$,*N*$^{22}$,*N*$^{23}$,*N*$^{24}$ (7)**: $BF_3$·$OEt_2$ (0.5 mL) was added to a degassed solution of dipyrromethane **6** (17.0 g, 18 mmol) and trimethylsilylpropynal (4.0 mL, 3.84 mmol) in $CH_2Cl_2$ (1.8 L) at 0 °C. After stirring at 0 °C for 1 h, 2,3-dichloro-5,6-dicyano-1,4-benzoquinone (DDQ; 7.0 g, 31 mmol) was added and the stirring was continued for 30 min at room temperature. The reaction mixture was concentrated and the product was purified by using flash chromatography on silica gel with $CH_2Cl_2$/hexane (1:1) as the eluent. This yielded the pure product as a purple solid (5.2 g, 28%). $^1$H NMR ($CDCl_3$, 200 MHz): $\delta = -2.20$ (s, 2H), 0.60 (s, 18H), 0.85–0.88 (m, 18H), 1.88–1.21 (m, 56H), 4.11 (m, 8H), 4.30 (m, 4H), 7.38 (s, 4H), 8.92 (d, $J = 4.4$ Hz, 4H), 9.58 ppm (d, $J = 4.4$ Hz, 4H); $^{13}$C NMR ($CDCl_3$, 50 MHz): $\delta = 0.3$, 14.1, 22.7, 26.2, 29.7, 32.0, 69.4, 71.0, 73.8, 100.7, 102.6, 106.9, 114.3, 121.9, 130.6, 131.6, 136.2, 138.1, 151.4 ppm; IR (KBr): $\tilde{\nu} = 2920$, 2852 ($CH_2$), 3316 (N–H), 2140 cm$^{-1}$ (C≡C); UV/Vis (THF): $\lambda_{max}$ ($\log \varepsilon \times 10^3$) = 434 (5.65), 444 (5.51), 583 (4.67), 680 nm (4.18 mol$^{-1}$ dm$^3$ cm$^{-1}$); HR-MALDI-MS: *m*/*z* calcd for $C_{138}H_{231}N_4O_6Si_2$ $[M+1]^+$: 2096.7432; found: 2096.7581.

**{5,15-Bis[3,4,5-tris(hexadecyloxy)phenyl]-10,20-bis[(trimethylsilyl)ethynyl]porphinato}-*N*$^{21}$,*N*$^{22}$,*N*$^{23}$,*N*$^{24}$-zinc(II) (8)**: A solution of Zn(OAc)$_2$·2H$_2$O (5.1 g, 26.7 mmol) in MeOH (50 mL) was added to a solution of **7** (5.1 g, 2.43 mmol) in $CHCl_3$ (100 mL) and the mixture was stirred at room temperature for 2 h. The crude reaction mixture was washed with $H_2O$ and dried over $Na_2SO_4$. The crude product was then purified by using flash chromatography on silica gel with $CH_2Cl_2$/hexane (1:1) as the eluent. This afforded a green solid (4.9 g, 95%). $^1$H NMR ($CDCl_3$, 200 MHz): $\delta = 0.60$ (s, 18H), 0.85–0.88 (m, 18H), 2.00–1.21 (m, 56H), 4.11–4.07 (m, 8H), 4.26–4.30 (m, 4H), 7.38 (s, 4H), 8.97 (d, $J = 4.4$ Hz, 4H), 9.64 ppm (d, $J = 4.4$ Hz, 4H); $^{13}$C NMR ($CDCl_3$, 50 MHz): $\delta = 0.3$, 14.1, 22.7, 26.2, 29.77, 30.6, 31.9, 69.3, 73.8, 100.8, 107.9, 111.0, 114.3, 122.6, 130.9, 132.6, 137.4, 137.7, 150.1, 151.1, 152.1 ppm; IR (KBr): $\tilde{\nu} =$ 2924, 2854 ($CH_2$), 2135 cm$^{-1}$ (C≡C); UV/Vis (THF): $\lambda_{max}$ ($\log \varepsilon \times 10^3$) = 438 (5.68), 449 (5.57), 583 (4.30), 636 nm (4.76 mol$^{-1}$ dm$^3$ cm$^{-1}$); HR-MALDI-MS: *m*/*z* calcd for $C_{138}H_{228}N_4O_6Si_2Zn$ $[M]^+$: 2157.6489; found: 2157.6633.

**{5,15-Bis[3,4,5-tris(hexadecyloxy)phenyl]-10,20-bis(ethynyl)porphinato}-*N*$^{21}$,*N*$^{22}$,*N*$^{23}$,*N*$^{24}$-zinc(II) (1)**: TBAF (490 mL, 1.0 M in THF, 0.49 mmol) was added to a solution of **8** (5.0 g, 2.3 mmol) in $CH_2Cl_2$ (300 mL). After 5 min, water (0.5 mL) was added and the mixture was evaporated to dryness. The crude product was purified by using flash chromatography on silica gel with $CH_2Cl_2$/hexane (1:1) as the eluent, to yield pure **1** as a green solid (4.6 g, 95%). $^1$H NMR ($CDCl_3$, 200 MHz): $\delta = 0.85$–0.88 (m, 18H), 2.00–1.21 (m, 56H), 4.11–3.95 (m, 8H), 4.16 (s, 2H), 4.30–4.20 (m, 4H), 7.35 (s, 4H), 9.05 (d, $J = 4.4$ Hz, 4H), 9.72 ppm (d, $J = 4.4$ Hz, 4H); $^{13}$C NMR ($CDCl_3$, 50 MHz): $\delta = 14.1$, 22.7, 26.1, 26.3, 29.4, 29.7, 30.5, 31.9, 69.2, 73.6, 83.9, 85.9, 100.0, 114.2, 122.7, 131.1, 133.0, 136.9, 137.7, 150.4, 150.9, 152.3 ppm; IR (KBr): $\tilde{\nu} = 2921$, 2852 ($CH_2$), 3311 (C≡C–H), 2095 cm$^{-1}$ (C≡C); UV/Vis (THF): $\lambda_{max}$ ($\log \varepsilon \times 10^3$) = 433 (5.50), 444 (5.54), 577 (4.40), 625 nm (4.55 mol$^{-1}$ dm$^3$ cm$^{-1}$); HR-MALDI-MS: *m*/*z* calcd for $C_{132}H_{212}N_4O_6Zn$ $[M]^+$: 2013.5698; found: 2013.5618.

**Polymer 2**: CuCl (1.02 g, 10.27 mmol) and TMEDA (1.55 mL, 10.27 mmol) were added to a vigorously stirred solution of **1** (0.25 g, 0.12 mmol) in $CH_2Cl_2$ (200 mL) and pyridine (1.9 mL) with dry air bubbled through it. After 30 min, the reaction mixture was washed repeatedly with water and the solvents were evaporated. The residue was dissolved in a minimum of chloroform/1% pyridine and precipitated into methanol. The precipitate was washed twice with methanol (2×50 mL) and vacuum dried to yield polymer **2** (0.23 g, 90%). $^1$H NMR ($CDCl_3$/1% [D$_5$]pyridine, 500 MHz): $\delta = 0.86$–0.81 (m, 18H), 2.00–1.19 (m, 56H), 4.19 (brs, 8H), 4.35 (brs, 4H), 7.42 (s, 4H), 9.08 (brs, 4H), 9.90 ppm (brs, 4H); $^{13}$C NMR ($CDCl_3$/1% [D$_5$]pyridine, 125 MHz): $\delta = 14.0$, 22.60, 22.64, 26.2, 26.4, 29.28, 29.34, 29.5, 29.7, 29.79, 29.84, 30.7, 31.8, 31.9, 69.6, 73.5, 100.2, 114.8, 123.7, 130.8, 133.1, 138.2, 150.3, 151.3, 153.1 ppm; IR (KBr): $\tilde{\nu} = 2924$, 2853 ($CH_2$), 2123 cm$^{-1}$ (C≡C); UV/Vis (THF): $\lambda_{max} =$ 468, 793 nm; GPC (THF): $M_n \approx 45700$ g mol$^{-1}$; $M_w \approx 88300$ g mol$^{-1}$.

## Acknowledgements

We would like to thank Andy Duft for help with the AFM measurements. Financial support for this work was provided by the Natural Science and Engineering Research Council of Canada (NSERC) Strategic Grants program, the Canada Foundation for Innovation (CFI), the Ontario Innovation Trust (OIT), and the Materials and Manufacturing Ontario Emerging Materials Knowledge Fund (EMK).

[1] A. Hirsch, *Angew. Chem.* **2002**, *114*, 1933–1939; *Angew. Chem. Int. Ed.* **2002**, *41*, 1853–1859.
[2] J. L. Bahr, J. M. Tour, *J. Mater. Chem.* **2002**, *12*, 1952–1958.
[3] S. Niyogi, M. A. Hamon, H. Hu, B. Zhao, P. Bhowmik, R. Sen, M. E. Itkis, R. C. Haddon, *Acc. Chem. Res.* **2002**, *35*, 1105–1113.
[4] D. Tasis, N. Tagmatarchis, V. Georgakilas, M. Prato, *Chem. Eur. J.* **2003**, *9*, 4001–4008.
[5] S. Banerjee, T. Hemraj-Benny, S. S. Wong, *Adv. Mater.* **2005**, *17*, 17–29.
[6] Y. P. Sun, K. F. Fu, Y. Lin, W. J. Huang, *Acc. Chem. Res.* **2002**, *35*, 1096–1104.
[7] Z. Yao, N. Braidy, G. A. Botton, A. Adronov, *J. Am. Chem. Soc.* **2003**, *125*, 16015–16024.
[8] Y. Q. Liu, A. Adronov, *Macromolecules* **2004**, *37*, 4755–4760.
[9] Y. Q. Liu, Z. L. Yao, A. Adronov, *Macromolecules* **2005**, *38*, 1172–1179.
[10] H. M. Li, F. O. Cheng, A. M. Duft, A. Adronov, *J. Am. Chem. Soc.* **2005**, *127*, 14518–14524.
[11] M. S. Strano, C. A. Dyke, M. L. Usrey, P. W. Barone, M. J. Allen, H. W. Shan, C. Kittrell, R. H. Hauge, J. M. Tour, R. E. Smalley, *Science* **2003**, *301*, 1519–1522.
[12] E. Zurek, J. Autschbach, *J. Am. Chem. Soc.* **2004**, *126*, 13079–13088.
[13] R. J. Chen, Y. Zhang, D. Wang, H. Dai, *J. Am. Chem. Soc.* **2001**, *123*, 3838–3839.
[14] N. Nakashima, Y. Tomonari, H. Murakami, *Chem. Lett.* **2002**, 638–639.
[15] P. Petrov, F. Stassin, C. Pagnoulle, R. Jerome, *Chem. Commun.* **2003**, 2904–2905.
[16] L. Liu, T. X. Wang, J. X. Li, Z. X. Guo, L. M. Dai, D. Q. Zhang, D. B. Zhu, *Chem. Phys. Lett.* **2003**, *367*, 747–752.
[17] S. A. Curran, P. M. Ajayan, W. J. Blau, D. L. Carroll, J. N. Coleman, A. B. Dalton, A. P. Davey, A. Drury, B. McCarthy, S. Maier, A. Strevens, *Adv. Mater.* **1998**, *10*, 1091–1093.

  

[18] A. B. Dalton, C. Stephan, J. N. Coleman, B. McCarthy, P. M. Ajayan, S. Lefrant, P. Bernier, W. J. Blau, H. J. Byrne, *J. Phys. Chem. B* **2000**, *104*, 10012–10016.
[19] A. Star, J. F. Stoddart, D. Steuerman, M. Diehl, A. Boukai, E. W. Wong, X. Yang, S. W. Chung, H. Choi, J. R. Heath, *Angew. Chem.* **2001**, *113*, 1771–1775; *Angew. Chem. Int. Ed.* **2001**, *40*, 1721–1725.
[20] F. J. Gomez, R. J. Chen, D. W. Wang, R. M. Waymouth, H. J. Dai, *Chem. Commun.* **2003**, 190–191.
[21] J. Chen, H. Y. Liu, W. A. Weimer, M. D. Halls, D. H. Waldeck, G. C. Walker, *J. Am. Chem. Soc.* **2002**, *124*, 9034–9035.
[22] J. Zhang, J. K. Lee, Y. Wu, R. W. Murray, *Nano Lett.* **2003**, *3*, 403–407.
[23] X. B. Wang, Y. Q. Liu, W. F. Qiu, D. B. Zhu, *J. Mater. Chem.* **2002**, *12*, 1636–1639.
[24] H. Murakami, T. Nomura, N. Nakashima, *Chem. Phys. Lett.* **2003**, *378*, 481–485.
[25] H. P. Li, B. Zhou, Y. Lin, L. R. Gu, W. Wang, K. A. S. Fernando, S. Kumar, L. F. Allard, Y. P. Sun, *J. Am. Chem. Soc.* **2004**, *126*, 1014–1015.
[26] J. Y. Chen, C. P. Collier, *J. Phys. Chem. B* **2005**, *109*, 7605–7609.
[27] T. Hasobe, S. Fukuzumi, P. V. Kamat, *J. Am. Chem. Soc.* **2005**, *127*, 11884–11885.
[28] A. Satake, Y. Miyajima, Y. Kobuke, *Chem. Mater.* **2005**, *17*, 716–724.
[29] D. M. Guldi, H. Taieb, G. M. A. Rahman, N. Tagmatarchis, M. Prato, *Adv. Mater.* **2005**, *17*, 871–875.
[30] K. Kadish, K. M. Smith, R. Guilard, *The Porphyrin Handbook*, Academic Press, New York, **1999**.
[31] H. L. Anderson, S. J. Martin, D. D. C. Bradley, *Angew. Chem.* **1994**, *106*, 711–713; *Angew. Chem. Int. Ed. Engl.* **1994**, *33*, 655–657.
[32] T. E. O. Screen, K. B. Lawton, G. S. Wilson, N. Dolney, R. Ispasoiu, T. Goodson, S. J. Martin, D. D. C. Bradley, H. L. Anderson, *J. Mater. Chem.* **2001**, *11*, 312–320.
[33] T. E. O. Screen, J. R. G. Thorne, R. G. Denning, D. G. Bucknall, H. L. Anderson, *J. Mater. Chem.* **2003**, *13*, 2796–2808.
[34] D. M. Guldi, G. M. A. Rahman, F. Zerbetto, M. Prato, *Acc. Chem. Res.* **2005**, *38*, 871–878.
[35] M. Kreyenschmidt, F. Uckert, K. Mullen, *Macromolecules* **1995**, *28*, 4577–4582.
[36] H. L. Anderson, *Chem. Commun.* **1999**, 2323–2330.
[37] Repeated filtration, washing, and resuspension of the polymer–nanotube complex resulted in the removal of some free polymer from solution at each iteration (as evidenced by some brown color in the filtrate) and consequent sedimentation of a small quantity of nanotubes after centrifugation. However, repetition of this process in excess of ten times still yielded a significant amount of soluble nanotube material, even though free polymer is removed at each iteration. This signifies an equilibrium between nanotube-bound and free polymer that is re-established at each resuspension step.
[38] It was found that the Zn–porphyrin polymer remained extremely stable to TFA in THF, with no observable demetalation. However, in noncoordinating solvents, such as dichloromethane, demetalation of polymer **2** occurs at elevated temperatures in the presence of TFA. Conversely, monomer **1** is more easily demetalated by TFA, with complete demetalation occurring within minutes in dichloromethane, and several days in THF at room temperature. The reason for this stability difference between the monomer and the polymer is currently unclear.

Received: March 3, 2006
Published online: May 2, 2006

  